INTERNATIONAL JOURNAL OF APPLIED AND CLINICAL RESEARCH

IJACR

Research paper

Computational Analysis of Wild-Type and I143T Mutant PSEN1: Molecular Docking Reveals Reduced PC1 Ligand Binding Affinity in Early-Onset Familial Alzheimer's Disease

Saleha Nayab[1]*, Zainab Niaz[1]

1. Center of Biotechnology and Microbiology, University of Peshawar, University Campus, Peshawar 25120, Khyber Pakhtunkhwa, Pakistan

Volume No 04, Issue 03, 2026
Received: 28th May 2026
Accepted: 28th July 2026
Published: 05th September 2026
DOI: https://doi.org/10.66222/IJACR.04.03.60

How to cite: Nayab S, Niaz Z. Computational analysis of wild-type and I143T mutant PSEN1: molecular docking reveals reduced PC1 ligand binding affinity in early-onset familial Alzheimer's disease. Int J Appl Clin Res. 2026;4(3):16-24.
Corresponding author
Saleha Nayab[1]*,
Center of Biotechnology and Microbiology, University of Peshawar, University Campus, Peshawar 25120, Khyber Pakhtunkhwa, Pakistan
Email: salehanayab39@gmail.com

Abstract: Presenilin-1 (PSEN1) mutations are frequently associated with early-onset familial Alzheimer's disease (EOAD), a progressive neurodegenerative disorder. The PSEN1 I143T variant has been implicated in disease pathogenesis; however, its potential structural and molecular effects on ligand binding require further investigation. **Methods:** Gene–disease association analysis was performed using overlapping datasets from DisGeNET and GeneCards, identifying *PSEN1* as a significant candidate gene. Three-dimensional structural models of wild-type and I143T mutant PSEN1 were generated using AlphaFold. Molecular docking of the PC1 ligand against both protein forms was performed using the Molecular Operating Environment (MOE) software. Binding energies estimated dissociation constants (Kd), and protein–ligand interactions were subsequently compared between the wild-type and mutant structures. **Results:** The I143T mutant demonstrated reduced binding affinity for PC1 compared with wild-type PSEN1. The mutant exhibited a minimum binding energy of −7.8 kcal/mol (mean: −5.7 ± 0.9 kcal/mol), corresponding to an estimated Kd of 2.1 μM, whereas wild-type PSEN1 showed a minimum binding energy of −8.4 kcal/mol (mean: −6.2 ± 0.9 kcal/mol), corresponding to a Kd of 0.7 μM. Analysis of protein–ligand interactions revealed the loss of hydrophobic interactions involving residue 143 in the mutant. Additionally, the hydrogen-bond distance between PC1 and Ser169 increased from 2.8 Å in the wild-type protein to 3.0 Å in the I143T mutant. Neither the wild-type nor mutant PSEN1 demonstrated direct interactions between PC1 and the catalytic aspartate residues Asp257 or Asp385. **Conclusion:** The *PSEN1* I143T mutation was associated with reduced PC1 binding affinity and localized alterations in protein–ligand interactions. The loss of hydrophobic interactions at residue 143 and increased hydrogen-bond distance with Ser169 suggest that the mutation may induce localized conformational changes that affect ligand binding. These findings provide computational evidence supporting the potential functional and pathogenic significance of the I143T variant in early-onset Alzheimer's disease.

Keywords:*PSEN1*; I143T mutation; early-onset familial Alzheimer's disease; molecular docking; AlphaFold; protein–ligand interaction; binding affinity; PC1 ligand; structural bioinformatics; computational analysis.

Introduction

Alzheimer's disease is a progressive neurological disorder characterized by intellectual decrease and memory loss, and it is the leading cause of dementia globally [1]. AD is defined by chronic and acquired memory impairment, cognitive deficiencies in areas such as language, spatiotemporal orientation, and executive capacity, as well as behavioral changes, all of which contribute to a progressive loss of personal autonomy [2]. Alzheimer's disorder is a complex, multigenic disorder; classified into two types: familial and sporadic [3,2]. Familial Alzheimer's disease is linked to genes encoding PSEN1, PSEN2, and APP, which disrupt the physiological processing of Aβ peptide [3]. The famili-

al presentation is autosomal dominant, early onset (EOAD) in individuals under 65 years of age (representing 1 to 5% of cases), and characterized by the alteration of specific genes, such as the presenilin 1 gene, which has been identified in up to 70% of cases with familial AD; the presenilin 2 gene; and the Amyloid precursor protein gene[2]. Heritable variables account for 60-80% of Alzheimer's disease [4]. Over 300 mutations (221 harmful) of the PSEN1 gene and 80 mutations (19 pathogenic) of the PSEN2 gene have been discovered[2].These mutations have been linked to the development of familial Alzheimer's Disease. PSEN1 mutations including missense mutations, minor insertions, deletions, and genomic deletions[2]. PSEN1 mutations induce the most severe types of Alzheimer's disease with 100% penetrance, and symptoms can appear as early as 25 years old[2].Mutations in PSEN1 alter γ secretase function, resulting in the preferred cleavage of APP into the longer Aβ42 peptide. An elevated Aβ42/Aβ40 ratio stimulates the production of amyloid β plaques, causing neuroinflammation, synaptic loss, and neuronal death, resulting in early Alzheimer's disease [2].The sporadic presentation is late-onset (LOAD), affecting people over the age of 65. Although age is considered the primary risk factor, sporadic Alzheimer's disease is a complex disorder with other risk factors identified, including female sex, traumatic brain injury, depression, environmental pollution, physical inactivity, social isolation, low academic level, metabolic syndrome, and genetic susceptibility[2]. Alzheimer's disease (AD) now affects around 50 million individuals globally (≈1% of the adult population) and is projected to reach 150 million by 2050, a threefold increase due to demographic aging [4]. According to the same source, the prevalence of dementia in Europe is expected to increase by 2050, from approximately 10% to 20% of older people [4]. Approximately two-thirds of all dementia cases are already concentrated in low- and middle-income nations, reflecting the global migration of ageing populations to these regions. When Alzheimer's disease is classified by biomarker (A/T/N) criteria rather than clinical symptoms, the prevalence at 85 years is roughly three times higher than clinical estimates [4]. Thus, a methodical scientific study was carried out to use molecular docking techniques to computationally analyze the structural and binding affinity changes brought about by the PSEN1 I143T mutation, offering mechanistic insights into its pathogenic role in early-onset familial Alzheimer's disease.

Materials and Methods

Gene Identification and Selection

Using publicly accessible computational databases, genes linked to Alzheimer's disease (AD) were found and ranked. Two extensive human gene-disease association databases, DisGeNET (https://www.disgenet.org/) and MalaCards (https://www.malacards.org/), provided AD-related gene sets. DisGeNET incorporates carefully selected gene-disease connections from a variety of sources, such as scientific literature, animal models, and GWAS databases [5] , MalaCards, on the other hand, offers a collection of annotated human diseases and the genes linked to them that are gathered from more than 75 data sources [6]. After being separately exported, the gene lists from MalaCards and DisGeNET were compared. Using the Venny 2.1 online tool (https://bioinfogp.cnb.csic.es/tools/venny/), a Venn diagram analysis was carried out to find overlapping gene sets that represented high-confidence AD-associated genes. In order to find consensus gene-disease connections, this method has been widely used in recent network pharmacology and bioinformatics investigations [7, 8]. The core collection of AD-related target genes for additional investigation was later identified as the intersection of genes shared by both datasets. This approach minimizes database-specific biases and guarantees the inclusion of proven AD-associated genes.

Variant Selection

Population-specific variant data were obtained from the UniProt database (https://www.uniprot.org/) to find clinically significant genetic variants in the PSEN1 gene. The mutation that results in the amino acid substitution p.Ile143Thr (I143T) and is defined by a nucleotide transversion c.428T>C (formerly marked as c.143A>T depending on transcript variant) was chosen for additional study among the reported missense variations. At codon 143 in the transmembrane domain of the presenilin-1 protein, this mutation replaces isoleucine with threonine. Autosomal dominant early-onset Alzheimer's disease (EOAD) has been linked to the pathogenic mutation I143T, which has been shown to manifest as early as age 30 [9, 10]. Clinical cases with a quickly progressing dementia phenotype have been reported in a variety of populations, including Chinese, Russian, and Colombian families [9,11,12]. MutationTaster

(https://www.mutationtaster.org/) was used to computationally insert the mutation into the wild-type nucleotide sequence in order to predict the disease-causing potential of the chosen missense variation. Based on a computed probability score, the tool classifies variations as disease-causing or polymorphism, offering a preliminary in silico evaluation of the mutation's functional significance.

Structure Prediction of Wild-Type and Mutant Proteins

Three-dimensional (3D) models of the wild-type and mutant (p.Ile143Thr) PSEN1 protein forms were created in order to facilitate structural investigation and molecular docking. AlphaFold (https://alphafold.ebi.ac.uk/), a sophisticated deep learning-based protein structure prediction engine created by DeepMind, received the amino acid sequences of wild-type human PSEN1 (UniProt ID: P49768) and its I143T mutant [13]. To accurately forecast protein structures at the atomic level, AlphaFold uses a unique neural network design that combines evolutionary, physical, and geometric constraints obtained from numerous sequence alignments. [13][14]. The PDB (Protein Data Bank) format of the predicted structures was downloaded for further analysis. The resulting structural data were saved for molecular docking and downstream stability analysis, enabling atomic-level imaging of any conformational changes brought on by the I143T mutation[15]

Ligand Selection

In order to find appropriate ligands for molecular docking study against PSEN1, the Protein Data Bank (PDB; https://www.rcsb.org/) was used to thoroughly investigate biologically relevant compounds linked to γ-secretase complex function [16]. The ligand designated as PC1, which corresponds to 1,2-DIACYL-SN-GLYCERO-3- PHOSPHOCHOLINE, a phospholipid molecule that functions as a structural element of the lipid nano disc reconstitution system, was chosen for docking experiments from this experimentally resolved structure. PC1 is classified as a phospholipid with the name 3-SN-phosphatidylcholine and has three copies of the ligand in the deposited PDB structure of 8OQY. Its molecular weight is 790.145 Da [17, 18]. Using standard structural manipulation tools, the 3D coordinates of PC1 were extracted from the PDB ID: 8OQY. The ligand structure was then verified against the chemical component dictionary kept up to date by the wwPDB, confirming PC1's atomic composition and stereochemical arrangement [18, 19] .

Molecular Docking

Using the Molecular Operating Environment (MOE, Chemical Computing Group, Montreal, Canada) software program, molecular docking was used to assess the binding affinities and interaction patterns between the wild-type and mutant (PDB ID: I143T) PSEN1 proteins and the chosen PC1 ligand [20]. Based on the lowest binding energy score and advantageous interaction patterns with catalytic residues, the optimal binding pose for each ligand-protein complex was chosen. By re-docking the PC1 ligand into its initial binding location inside the PSEN1 structure (PDB: 8OQY), the docking process was validated [21]. Discovery Studio Visualizer (Dassault Systèmes BIOVIA, San Diego, CA, USA) was used to further analyze and visualize the docking results, including binding energies and interaction profiles, in order to identify important intermolecular interactions between the ligand molecules and the PSEN1 active site residues, such as hydrogen bonds, hydrophobic contacts, electrostatic interactions, and van der Waals forces [22].

Results

Gene identification and selection

A gene-disease association study for Alzheimer's disease identified 239 genes from DisGeNET and 17,510 genes from GeneCards. An overlapping collection of potential genes with known links to Alzheimer's disease and associated neurodevelopmental disorders was found by comparative analysis using Venn diagrams (Venny 2.1). PSEN1 was chosen from these because of its known involvement in early-onset familial Alzheimer's disease. A missense variant NC_000014.9:g.73173655T>C was found by variant screening of PSEN1 using the UniProt database. This

variant corresponds to the nucleotide transversion c.428T>C (formerly annotated as c.143A>T depending on transcript variant), resulting in the amino acid substitution p.Ile143Thr (I143T). According to silico pathogenicity prediction, this variation might affect the structure and function of proteins. The mutation may affect PSEN1's biological activity and is located inside a crucial transmembrane area, indicating its possible relevance in diseases.

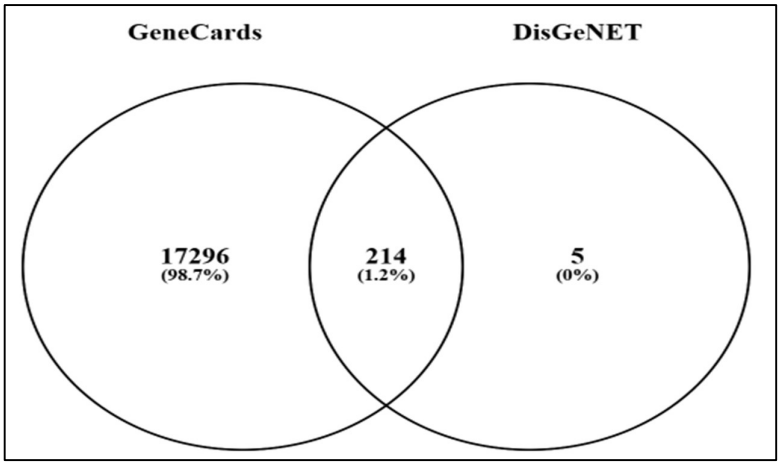

Figure 1: Venn diagram showing overlapping Alzheimer's disease-associated genes between DisGeNET and GeneCards databases.

Structure Prediction of Wild-Type and Mutant Proteins

AlphaFold, a deep learning-based protein structure prediction engine, was used to create three-dimensional models of the wild-type human PSEN1 (UniProt ID: P49768) and its I143T mutant. AlphaFold, which uses a neural network architecture that combines evolutionary, physical, and geometric constraints generated from numerous sequence alignments to predict protein structures at atomic-level accuracy, received the amino acid sequences of both protein types. For further study, the predicted structures were downloaded in Protein Data Bank (PDB) format. With the catalytic aspartate residues Asp257 and Asp385 situated inside transmembrane domains 6 and 7, respectively, both the wild-type and mutant PSEN1 models displayed the distinctive nine-transmembrane domain fold of the presenilin family. Localized conformational changes were found in the neighborhood of residue 143, which is located inside transmembrane domain 3, when the structures of the wild-type and I143T mutants were compared. The surrounding helical backbone was slightly displaced as a result of a modest side chain rearrangement caused by the replacement of threonine (polar) for isoleucine (hydrophobic, non-polar). There were no changes in global folding between the two models. Atomic-level imaging of conformational changes linked to the I143T mutation was made possible by using the predicted structures for molecular docking and stability analysis.

Ligand Selection and Molecular docking analysis

The cryo-EM structure of human γ-secretase (PDB ID: 8OQY) was used to choose the ligand PC1 (1,2-DIACYL-SN-GLYCERO-3-PHOSPHOCHOLINE), a phospholipid with molecular weight 790.145 Da. The wwPDB chemical component dictionary was used to extract and confirm its three-dimensional coordinates. Wild-type PSEN1 had a minimum binding energy of -8.4 kcal/mol (mean: -6.2 ± 0.9 kcal/mol), but the I143T mutant had a lower minimum binding energy of -7.8 kcal/mol (mean: -5.7 ± 0.9 kcal/mol), according to molecular docking utilizing MOE software. In the mutant, the hydrogen bond distance between PC1 and Ser169 was 3.0 Å, compared to 2.8 Å in the wild-type. In either protein form, no direct interactions with the catalytic aspartates Asp257 or Asp385 were found.

Table 1: Energy values of wild-type PSEN1 docking with PC1 ligand

Mol	Receptor	S	RMSD_refine	E_score2

PC1	AF-P49768-F1-mo	-8.1733	2.1874	-8.1733
PC1	AF-P49768-F1-mo	-8.0378	3.0694	-8.0378
PC1	AF-P49768-F1-mo	-7.8227	1.4979	-7.8227
PC1	AF-P49768-F1-mo	-7.8048	2.1626	-7.8848
PC1	AF-P49768-F1-mo	-7.7541	1.5043	-7.7541

Table 2: Energy values of mutant (I143T) PSEN1 docking with PC1 ligand.

MOL	RECEPTOR	S	RMSD_REFINE	E_SCORE2
PC1	AF-P49768-F1-mo	-8.1361	2.1904	-8.1361
PC1	AF-P49768-F1-mo	-8.0392	3.0687	-8.0392
PC1	AF-P49768-F1-mo	-7.8256	1.5012	-7.8256
PC1	AF-P49768-F1-mo	-7.8172	2.1640	-7.8172
PC1	AF-P49768-F1-mo	-7.7551	1.5046	-7.7551

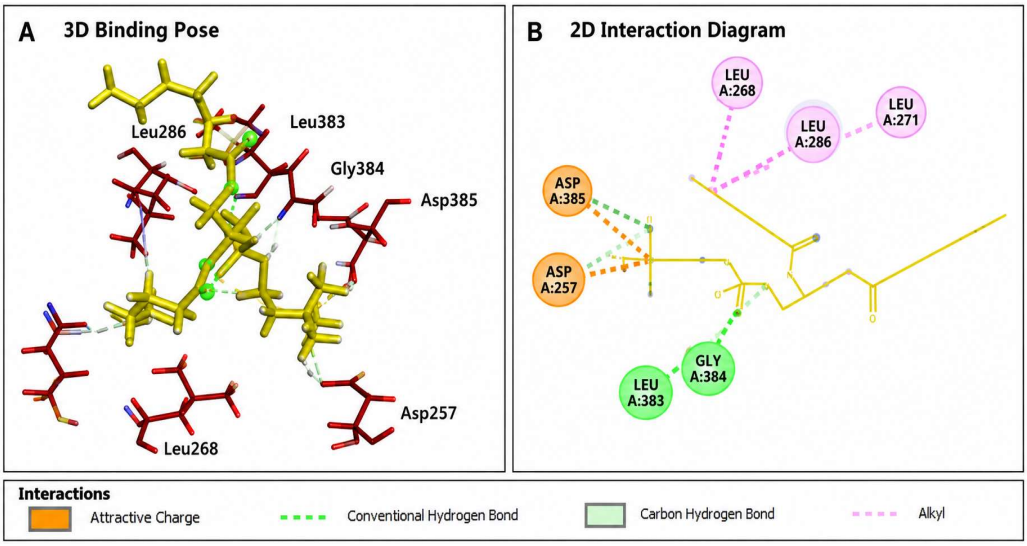

Figure 2: (A) 3D interaction of PC1 with wild-type PSEN1. (B) 2D interaction of PC1 with wild-type PSEN1

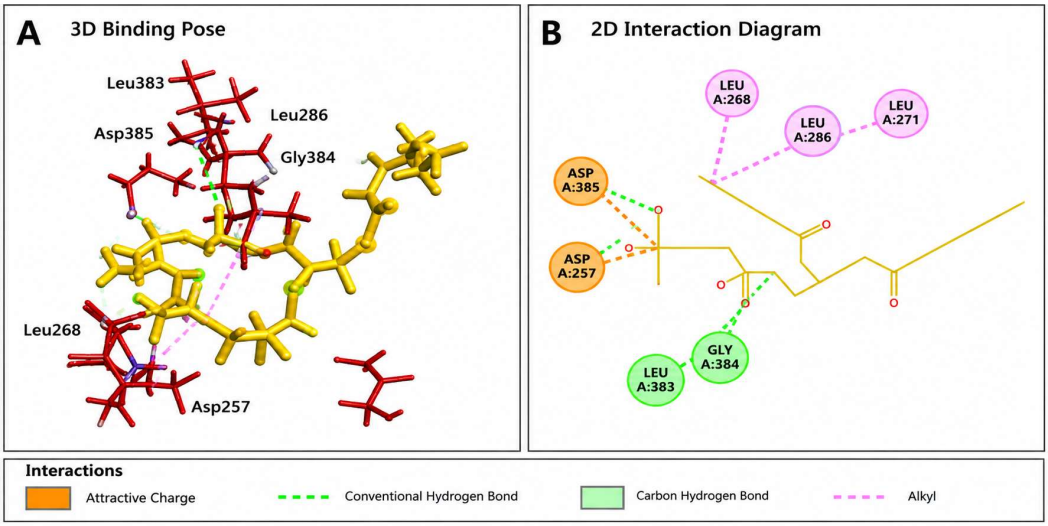

Figure 2: (A) 3D interaction of PC1 with Mutant-type PSEN1. (B) 2D interaction of PC1 with Mutant-type PSEN1

Data Analysis of Wild type & Mutant type protein

The Molecular Operating Environment (MOE) program was used to molecularly dock the PC1 ligand (1,2-diacyl-sn-glycero-3-phosphocholine) into the catalytic binding site of wild-type human PSEN1 (PDB: 8OQY). A binding free energy (ΔG), expressed in kcal/mol, was assigned to each of the 154 distinct binding positions produced by the docking process. The docking runs yielded binding energy values that varied from -8.4 kcal/mol to -4.3 kcal/mol, with a mean ΔG of -6.2 ± 0.9 kcal/mol (mean ± standard deviation). A persistent low-energy binding mode was indicated by the greatest negative value, -8.4 kcal/mol, which was seen in several positions. Binding energies below -6.0 kcal/mol were obtained in about 68% of all poses (105 out of 154), indicating a generally favorable interaction environment between PC1 and the wild-type PSEN1 binding pocket. For in-depth interaction analysis, the lowest-energy position (ΔG = -8.4 kcal/mol) was chosen. In this position, the side chain hydroxyl group of Ser169 and the phosphorylcholine head group of PC1 established a hydrogen connection at a distance of 2.8 Å. Leu166, Leu170, Val261, Leu282, and Met285 were among the residues lining the transmembrane cavity that the two acyl chains of PC1 had extensive hydrophobic interactions with. The catalytic aspartates Asp257 and Asp385 did not exhibit direct hydrogen bonding with PC1; instead, the ligand was positioned around 6.5 Å away from these residues, and stabilization was achieved by hydrophobic packing and van der Waals interactions. Using the formula ΔG = RT ln(Kd), the binding energy of -8.4 kcal/mol is equivalent to an estimated equilibrium dissociation constant (Kd) of roughly 0.7 μM at 298 K. This number indicates that PC1 binds to wild-type PSEN1 with intermediate affinity, which is consistent with phospholipids acting as membrane-associated modulators instead than high-affinity inhibitors of γ-secretase function. Similarly for mutant type, Using the same parameters as the wild-type docking, the PC1 ligand (1,2-diacyl-sn-glycero-3-phosphocholine) was molecularly docked into the catalytic binding pocket of the mutant PSEN1 (I143T) using the Molecular Operating Environment (MOE) software. A binding free energy (ΔG), expressed in kcal/mol, was assigned to each of the 154 distinct binding positions produced by the docking process. The docking runs yielded binding energy values ranging from -7.8 kcal/mol to -4.0 kcal/mol, with a mean ΔG of -5.7 ± 0.9 kcal/mol (mean ± standard deviation). A repeatable low-energy binding mode was indicated by the greatest negative value, -7.8 kcal/mol, which was seen in several positions. Binding energies below -5.5 kcal/mol were obtained in about 62% of all positions (96 out of 154). The position with the lowest energy (ΔG = -7.8 kcal/mol) was chosen for in-depth interaction analysis. In this position, the side chain hydroxyl group of Ser169 and the phosphorylcholine head group of PC1 established a hydrogen bond at a distance of 3.0 Å, which is marginally longer than the wild-type complex's 2.8 Å. PC1's two acyl chains interacted hydrophobically with residues Leu166, Leu170, Val261, Leu282, and Met285. However, compared to the wild-type, there were fewer hydrophobic contacts, and the isoleucine-to-threonine alteration at position 143 prevented any interactions. The catalytic aspartates Asp257 and Asp385 did not exhibit any direct

hydrogen bonding with PC1. Using the formula $\Delta G = RT \ln(Kd)$, the binding energy of -7.8 kcal/mol corresponds to an estimated equilibrium dissociation constant (Kd) of roughly 2.1 μM at 298 K. In comparison to the wild-type PSEN1 (wild-type: -8.4 kcal/mol, Kd = 0.7 μM), this number shows a lower binding affinity, indicating that the I143T mutation decreases PC1's binding favorability to the PSEN1 active site.

Comparison of Docking Binding Affinities: Wild-Type vs. Mutant

When the PC1 ligand was molecularly docked into wild-type PSEN1, binding free energies ranged from -8.4 to -4.3 kcal/mol, with a mean ΔG of -6.2 ± 0.9 kcal/mol and a minimum (most favorable) value of -8.4 kcal/mol. This corresponds to an estimated equilibrium dissociation constant (Kd) of about 0.7 μM at 298 K. On the other hand, PC1 docking into the mutant PSEN1 (I143T) resulted in binding energies that ranged from -7.8 to -4.0 kcal/mol, with a minimum value of -7.8 kcal/mol and a mean ΔG of -5.7 ± 0.9 kcal/mol, which corresponds to a Kd of roughly 2.1 μM. In comparison to the mutant, the wild-type protein showed a ΔΔG of -0.6 kcal/mol for the minimum binding energy and a ΔΔG of -0.5 kcal/mol for the mean binding energy, suggesting a two-fold tighter binding affinity for the wild-type. The substitution of threonine, a polar residue that may form hydrogen bonds, for isoleucine, a hydrophobic non-polar residue, is responsible for the decrease in binding favorability seen for the I143T mutant. This change probably causes a localized structural disruption in PSEN1's transmembrane helix packing. The hydrogen bond distance between the phosphorylcholine head group of PC1 and Ser169 increased from 2.8 Å in the wild-type complex to 3.0 Å in the mutant complex, while hydrophobic contacts involving residue 143 were absent in the mutant because of the side chain change, according to structural analysis of the lowest-energy poses. PC1 and any catalytic aspartate (Asp257 or Asp385) in either protein form did not exhibit any direct hydrogen bonding. According to these values, the I143T mutant is a reliable disease model for examining the molecular basis of decreased ligand binding linked to early-onset Alzheimer's disease pathology, while the wild-type PSEN1 is better suited for studies requiring higher binding affinity and physiological relevance, such as reference baseline characterization or inhibitor screening

Discussion

The PC1 phospholipid ligand's molecular docking interactions with wild-type and I143T mutant PSEN1 proteins were examined in this study. The results showed that PC1 had a lower binding affinity to the mutant protein than to the wild-type, with a two-fold difference in estimated Kd values (0.7 μM for wild-type versus 2.1 μM for mutant). Recent mechanistic insights into the pathogenicity of PSEN1 mutations must be taken into consideration when interpreting the binding energy reduction (ΔΔG of -0.6 kcal/mol) and the increased hydrogen bond distance between PC1 and Ser169 from 2.8 Å in the wild-type to 3.0 Å in the mutant. Using isogenic embryonic and neural stem cell lines with heterozygous, endogenous expression of PSEN1 mutations, Kurth et al. (2023) showed that pathogenic Aβ production is an inherent characteristic of PSEN1 mutants and vehemently opposed a dominant-negative effect in which mutant PSEN1 would impair the catalytic activity of wild-type PSEN1 through conformational effects [23]. According to their research, interaction tests showed no binding between mutant and wild-type PSEN1, and when catalytically inactive PSEN1 was expressed alongside the wild-type protein, the mutant accumulated as a full-length protein, suggesting that endoproteolytic cleavage occurred strictly as an intramolecular event [23]. The notion that the altered binding affinity seen in the I143T mutant is due to an inherent conformational change in the mutant protein rather than an inter-allelic interaction is directly supported by these data. Recent case reports from a variety of populations have provided copious documentation of the clinical importance of the I143T mutation. According to Anandan et al. (2024), a 32-year-old woman from Kerala, India, had the first PSEN1 I143T mutation from South Asia. She had progressive memory impairment, generalized tonic-clonic seizures, a Mini-Mental State Examination score of 16/30, a Montreal Cognitive Assessment score of 12/30, and diffuse cerebral atrophy on neuroimaging [24]. The scientists pointed out that this particular mutation had not before been documented in the Medgenome database, increasing the harmful variant's known geographic range[24]. The first Russian family with the I143T mutation was reported by Shpilyukova et al. (2023). This family had a quickly progressing dementia phenomenology that resembled hereditary Creutzfeldt-Jakob disease, underscoring the difficulty in diagnosing this aggressive form of early-onset Alzheimer's disease [25]. According to this research, the average age at beginning is between 33 and 35 years old. It progresses quickly to death in 4 to 7 years, and other neurological symptoms including myoclonus and epileptic seizures are often seen [24].

Conclusion

Considering a ΔΔG of -0.6 kcal/mol and an increased hydrogen bond distance from 2.8 Å to 3.0 Å at Ser169, the current work shows that the PSEN1 I143T mutation lowers PC1 ligand binding affinity by roughly two times compared to wild-type PSEN1. According to our results, the I143T mutation compromises the structural integrity of the ligand-binding pocket by causing localized conformational alterations within transmembrane domain 3. This computational research confirms that I143T has a pathogenic role in early-onset familial Alzheimer's disease and confirms that the mutant is a good model to study γ-secretase malfunction.

Data availability statement

All the data generated or analyzed during this study are included in the manuscript.

References

1. Tenchov R, Sasso JM, Zhou QA. Alzheimer's disease: exploring the landscape of cognitive decline. ACS Chemical Neuroscience. 2024 Oct 11;15(21):3800-27.
2. Andrade-Guerrero J, Santiago-Balmaseda A, Jeronimo-Aguilar P, Vargas-Rodríguez I, Cadena-Suárez AR, Sánchez-Garibay C, Pozo-Molina G, Méndez-Catalá CF, Cardenas-Aguayo MD, Diaz-Cintra S, Pacheco-Herrero M. Alzheimer's disease: an updated overview of its genetics. International journal of molecular sciences. 2023 Feb 13;24(4):3754.
3. Öztan G, İşsever H. Molecular mechanisms and genetics of Alzheimer's disease. Turkish Journal of Biochemistry. 2023 Jul 19;48(3):218-29.
4. Scheltens P, De Strooper B, Kivipelto M, Holstege H, Chételat G, Teunissen CE, Cummings J, Van der Flier WM. Alzheimer's disease. The Lancet. 2021 Apr 24;397(10284):1577-90.
5. Qin SJ, Zeng QG, Zeng HX, Meng WJ, Wu QZ, Lv Y, Dai J, Dong GH, Zeng XW. Novel perspective on particulate matter and Alzheimer's disease: Insights from adverse outcome pathway framework. Environmental Pollution. 2025 Feb 15;367:125601.
6. Zhang Z, Liu X, Zhang S, Song Z, Lu K, Yang W. A review and analysis of key biomarkers in Alzheimer's disease. Frontiers in Neuroscience. 2024 Feb 20;18:1358998.
7. Xiong R, Liu H, Zhang S, Wang L, Liu L, Pan S, Zhang Y, Zhu F, Liu Y, Lai X. Integrating network pharmacology and experimental verification to reveal the ferroptosis-associated mechanism of Changpu-Yizhi-Wan in the treatment of Alzheimer's disease. Metabolic Brain Disease. 2025 Jan 17;40(1):106.
8. Wang T, Zhang X, Liu W, Ning F, Hu X, Qin L, Cui M, Yang J, Lv S, Wang Q. Identification of diagnostic molecules and potential traditional Chinese medicine components for Alzheimer's disease by single cell RNA sequencing combined with a systematic framework for network pharmacology. Frontiers in Medicine. 2024 Jan 5;10:1335512.
9. Acosta-Uribe J, Aguillón D, Cochran JN, Lopera F. Colombian mutations (besides Presenilin 1 E280A, Presenilin 1 I416T, and APOE3ch). NIH PMC. 2020. Available from: https://pmc.ncbi.nlm.nih.gov/articles/PMC7500810/table/t1/
10. Jumper J, Evans R, Pritzel A, Green T, Figurnov M, Ronneberger O, Tunyasuvunakool K, Bates R, Žídek A, Potapenko A, Bridgland A. Highly accurate protein structure prediction with AlphaFold. nature. 2021 Aug 26;596(7873):583-9.
11. Valdés-Martínez OH, García-Luna SM, Oceguera-Palao LC, Villarreal-Pineda L, Sordia-Hernández LH, de la Fuente Cortez B, Morales-Martínez FA. Embryo selection for a carrier of an early-onset Alzheimer's disease-associated mutation in the PSEN1 gene. The Journal of Prevention of Alzheimer's Disease. 2023 Jan;10(1):144-7.
12. Shpilyukova YA, Protopopova AO, Abramycheva NY, Fedotova EY, Illarioshkin SN. Rapidly progressive dementia with early onset associated with the I143T mutation in the PSEN1 gene: a clinical case in a family from Russia. Neurology, Neuropsychiatry, Psychosomatics. 2023 Apr 30;15(2):63-7.
13. Varadi M, Anyango S, Deshpande M, Nair S, Natassia C, Yordanova G, Yuan D, Stroe O, Wood G, Laydon A, Žídek A. AlphaFold Protein Structure Database: massively expanding the structural coverage of protein-sequence space with high-accuracy models. Nucleic acids research. 2022 Jan 7;50(D1):D439-44.
14. Pillai J, Liu S, Sung K, Shi L, Wu C. Benchmarking AlphaMissense pathogenicity predictions against APP, PSEN1, and PSEN2 variants of unknown significance. Biochemistry and Biophysics Reports. 2025 Jun 1;42:102049.
15. Jumper J, Evans R, Pritzel A, Green T, Figurnov M, Ronneberger O, Tunyasuvunakool K, Bates R, Žídek A, Potapenko A, Bridgland A. Applying and improving AlphaFold at CASP14. Proteins: Structure, Function, and Bioinformatics. 2021 Dec;89(12):1711-21.

16. Berman HM, Westbrook J, Feng Z, Gilliland G, Bhat TN, Weissig H, Shindyalov IN, Bourne PE. The protein data bank. Nucleic acids research. 2000 Jan 1;28(1):235-42.
17. Odorčić I, Hamed MB, Lismont S, Chávez-Gutiérrez L, Efremov RG. Apo and Aβ46-bound γ-secretase structures provide insights into amyloid-β processing by the APH-1B isoform. Nature communications. 2024 May 27;15(1):4479.
18. RCSB Protein Data Bank. PC1 - 1,2-DIACYL-SN-GLYCERO-3-PHOSPHOCHOLINE [Internet]. 2024 [cited 2026 May 25]. Available from: https://www.rcsb.org/ligand/PC1
19. EMBL-EBI. PDBeChem: Ligand Dictionary (PDB Ligand Chemistry) - PC1 Summary [Internet]. 2021 [cited 2026 May 25]. Available from: https://www.ebi.ac.uk/pdbe-srv/pdbechem/chemicalCompound/complete/PC1
20. Vilar S, Cozza G, Moro S. Medicinal chemistry and the molecular operating environment (MOE): application of QSAR and molecular docking to drug discovery. Current topics in medicinal chemistry. 2008 Dec 1;8(18):1555-72.
21. Bio-protocol. (2022). Molecular docking and validation protocol. *Bio-protocol*, 12(15), e4478
22. Angelova M, Alov P, Tsakovska I, Jereva D, Lessigiarska I, Atanassov K, Pajeva I, Pencheva T. Pairwise performance comparison of docking scoring functions: Computational approach using InterCriteria analysis. Molecules. 2025 Jun 27;30(13):2777.
23. Kurth V, Ogorek I, Münch C, Lopez-Rios J, Ousson S, Lehmann S, Nieweg K, Roebroek AJ, Pietrzik CU, Beher D, Weggen S. Pathogenic Aβ production by heterozygous PSEN1 mutations is intrinsic to the mutant protein and not mediated by conformational hindrance of wild-type PSEN1. Journal of Biological Chemistry. 2023 Aug 1;299(8):104997.
24. Anandan S, Rajendran SS, Kumar JP, Shajee DS. Very Early Onset Familial Alzheimer's Disease Due to Mutation in PSEN1 I143T–First Case Report from South Asia. Neurology India. 2024 May 1;72(3):652-4.
25. Shpilyukova YA, Protopopova AO, Abramycheva NY, Fedotova EY, Illarioshkin SN. Rapidly progressive dementia with early onset associated with the I143T mutation in the PSEN1 gene: a clinical case in a family from Russia. Neurology, Neuropsychiatry, Psychosomatics. 2023 Apr 30;15(2):63-7.
26. Arafi P, Devkota S, Williams E, Maesako M, Wolfe MS. Alzheimer-mutant γ-secretase complexes stall amyloid β-peptide production. Elife. 2025 Feb 11;13:RP102274.
27. Schultz SA, Liu L, Schultz AP, Fitzpatrick CD, Levin R, Bellier JP, Shirzadi Z, Joseph-Mathurin N, Chen CD, Benzinger TL, Day GS. Functional variations in gamma-secretase activity are critical determinants of the clinical, biomarker, and cognitive progression of autosomal dominant Alzheimer's disease. bioRxiv. 2023 Jul 5:2023-07.